

## IMPROVED OPTICAL SPECTROPHOTOMETRY OF SUPERNOVA REMNANTS IN M33<sup>1</sup>

WILLIAM P. BLAIR

Harvard-Smithsonian Center for Astrophysics

AND

ROBERT P. KIRSHNER<sup>2</sup>

Department of Astronomy, University of Michigan

Received 1984 June 28; accepted 1984 September 6

### ABSTRACT

We present spectrophotometry of 12 supernova remnants in the galaxy M33. The spectra generally cover the wavelength range 4750–7000 Å at a resolution of 7 Å. These data are analyzed in light of recent shock model calculations and are used to investigate abundance gradients in M33. Gradients in nitrogen and sulfur abundances are clearly present and are similar to those found in our own Galaxy. The situation for oxygen is complicated by the probable presence of low shock velocity remnants in the sample, which particularly affects the oxygen abundance determinations. These results are compared with the abundance gradients from H II regions in M33 and are found to be similar. The [S II]  $\lambda\lambda 6717/\lambda\lambda 6731$  ratio is well observed for each of the remnants, and a calculation using the latest atomic parameters is employed to obtain electron densities from this line ratio. These densities are used with a pressure equilibrium argument to estimate the initial explosion energy for each remnant. As with other samples of remnants, this energy appears to be a function of the present diameter of the remnants. We investigate evolutionary models for the M33 remnants and find that the distribution of the number of remnants with diameter is consistent with free expansion of the remnants to diameters of  $\sim 26$  pc. However, the results may also be consistent with Sedov evolution if the ranges of initial supernova energies and surrounding interstellar medium densities are large enough.

*Subject headings:* galaxies: individual — nebulae: abundances — nebulae: supernova remnants — spectrophotometry

### 1. INTRODUCTION

Improvements in techniques and detectors over the past decade have made it feasible to study supernova remnants (SNRs) in other galaxies. Extragalactic SNR candidates can be identified on interference-filter photographic plates: Since remnants usually show much stronger emission lines of [S II]  $\lambda\lambda 6717, 6731$  relative to H $\alpha$  than do photoionized regions, photographs in these emission lines allow the remnants to be distinguished from H II regions. This technique has now been used on many nearby galaxies (Mathewson and Clarke 1972; D'Odorico, Dopita, and Benvenuti 1980; Blair, Kirshner, and Chevalier 1981), the largest samples being found in the Magellanic Clouds, M31, and M33. The SNR candidates beyond the Magellanic Clouds are usually confirmed by obtaining optical spectra (Dopita, D'Odorico, and Benvenuti 1980; Blair, Kirshner, and Chevalier 1982) or radio measurements (Goss *et al.* 1980; D'Odorico, Goss, and Dopita 1982; Dickel *et al.* 1982; Dickel and D'Odorico 1984).

Recently, the X-ray surveys of the Magellanic Clouds (Long, Helfand, and Grabelsky 1981; Seward and Mitchell 1981) have confirmed known optical SNR candidates and have enlarged the lists of candidates. Subsequent optical and radio work at the X-ray positions (Mills *et al.* 1982; Mathewson *et al.* 1983, 1984) has brought the confirmed SNR totals to 27 for the Large Magellanic Cloud (LMC) and six for the Small Magellan-

ic Cloud (SMC). X-ray surveys of M33 and M31 have not been sensitive enough to detect most of the SNRs, although a few isolated detections have been obtained (cf. Markert and Rallis 1983 for M33 and van Speybroeck *et al.* 1979 for M31).

Extragalactic SNR samples are important for a number of reasons. SNR evolution can best be studied when the relative sizes of the remnants in a sample can be compared confidently. Because the distances to individual galactic SNRs are so uncertain, it is difficult to study remnant evolution with the local sample. A sample of SNRs in another galaxy are all effectively at the same distance and can be compared directly. This has been done for SNRs in the Magellanic Clouds (Dennefeld 1978; Mathewson *et al.* 1983) and M31 (Dennefeld and Kunth 1981; Blair, Kirshner, and Chevalier 1981).

Extragalactic remnants can also be used as probes of the galaxies in which they reside. With the advent of sophisticated shock wave modeling programs (Dopita 1977; Raymond 1979; Shull and McKee 1979; Dopita *et al.* 1984), it has become possible to extract some abundance information from SNR spectra. Abundance gradients from SNRs have been derived for M33 (Dopita, D'Odorico, and Benvenuti 1980) and M31 (Dennefeld and Kunth 1981; Blair, Kirshner, and Chevalier 1982) and in our own Galaxy (Binette *et al.* 1983; Fesen, Blair, and Kirshner 1985). These results generally confirm the abundance gradients found from H II regions, especially for nitrogen. The uncertainties in each method are considerable, but the convergence of results provides confidence in each technique.

The published spectra of the dozen or so SNRs each in M33 (Dopita, D'Odorico, and Benvenuti 1980) and M31 (Blair, Kirshner, and Chevalier 1982) are of sufficient quality to confirm the SNR identifications, but many of these spectra

<sup>1</sup> This article reports observations obtained at the Multiple Mirror Telescope Observatory, which is operated jointly by the Smithsonian Institution and the University of Arizona.

<sup>2</sup> Guest Observer, Kitt Peak National Observatory, operated by the Association of Universities for Research in Astronomy, Inc., under contract with the National Science Foundation.

have relatively low signal-to-noise ratios. Also, the resolution in these spectra is low, and the density-sensitive lines of [S II]  $\lambda\lambda 6717, 6731$  are often blended. We have embarked on a program to obtain higher quality spectra of the M33 and M31 SNRs in order to permit a more careful analysis of SNR evolution and abundance gradients in these galaxies.

This paper presents spectrophotometry of 12 M33 SNRs, including one remnant which has not been previously observed. The observational data are presented in § II and compared with previous M33 SNR data. Abundances and abundance gradients are derived and discussed in § III, and possible evolutionary trends within the M33 SNR sample are presented in § IV. Conclusions are given in § V, along with suggestions for future observations.

## II. OBSERVATIONS AND COMPARISON WITH PREVIOUS DATA

The SNRs in M33 range in angular size from  $\sim 2''$  to  $\sim 20''$ , with the larger remnants often having quite low surface brightnesses. (Note: at an assumed distance of 720 kpc,  $1'' = 3.6$  pc.) We have used several telescopes and spectrometers to obtain our optical data, optimizing the slit sizes to the object sizes when possible. The observations are summarized in Table 1, where the remnants are identified using the catalog numbers from D'Odorico, Dopita, and Benvenuti (1980). The remnants that we observed are the same ones studied by Dopita, D'Odorico and Benvenuti (1980), with the exclusion of M33-14 and the inclusion of M33-1, for which no previous spectrum exists.

Initially, two M33 remnants were observed at Kitt Peak National Observatory (KPNO) using the 2.1 m telescope and intensified image dissector scanner (IIDS) to investigate the feasibility of obtaining spectra with higher signal-to-noise ratios at higher resolution. Most of the remaining spectra were

obtained at Mount Hopkins using either the 1.5 m telescope of the F. L. Whipple Observatory (FLWO) and an intensified Reticon spectrometer (the "Z-machine"; see Latham 1982) or the Multiple Mirror Telescope (MMT) and the MMT spectrograph (which is also an intensified Reticon detector). All three of these instruments have dual apertures for simultaneous sky subtraction. One remnant was observed at the McGraw-Hill Observatory with the 1.3 m telescope and the Mark II intensified Reticon spectrograph (similar to the instrument described by Sackett and Hiltner 1976). This instrument has a single aperture, and sky measurements are made by chopping to a sky location about  $60''$  away every 15 s. Most of the spectra cover the region from about H $\beta$  to  $\sim 7000$  Å with  $\sim 7$  Å resolution (see Table 1).

The small, high surface brightness remnants were visible on the television guider at the MMT, but in general the SNRs could not be seen and the slits were positioned by offsetting from nearby stars. The observations were reduced to flux versus wavelength for each object by the following procedures. Sky and galaxy background were subtracted from each object, and atmospheric extinction was removed by using average extinction coefficients. Flux calibrations were obtained from observations of several Oke (1974) white dwarf stars each night, and wavelength calibrations were derived from observations of comparison lamps. Several representative reduced spectra from the various systems are shown in Figure 1.

Since these data were obtained at different sites and under different conditions, they are not of uniform quality. However, comparison of results from individual standard stars on each night are usually consistent to within  $\pm 20\%$  ( $\pm 35\%$  in the most extreme cases), which should reflect the errors expected in the absolute calibrations. We estimate that the relative fluxes from red end to blue end within a given spectrum are known to

TABLE 1  
LOG OF OBSERVATIONS

Object	Date UT	Telescope/ Instrument	Aperture (arcsec)	Integration Time (s)	Spectral Coverage (Å)	Resolution (Å)
M33-2	1981 Aug 28	KPNO 2.1 m IIDS	8	2400	5800-7100	8
M33-5	1981 Aug 28	KPNO 2.1 m IIDS	8	2400	5800-7100	8
M33-18	1982 Sep 26	FLWO 1.5 m Z-machine	$6 \times 12.6$	3000	4500-7000	7
M33-9	{1982 Sep 29 1982 Oct 1}	McG-H 1.3 m Mark II	4	{1800 1800}	4100-7000	12
M33-6	1982 Oct 11	MMT	$1 \times 2.6$	2400	4750-7400	6
M33-7	1982 Oct 11	MMT Spec.	$1 \times 2.6$	2400	4750-7400	6
M33-8	1982 Oct 11	MMT Spec. MMT	$1 \times 2.6$	3600	4750-7400	6
M33-11	1982 Oct 11	MMT Spec. MMT	$1 \times 2.6$	2400	4750-7400	6
M33-4	1982 Oct 11	MMT Spec. MMT	$1 \times 2.6$	2400	4750-7400	6
M33-15	1982 Oct 12	MMT Spec. MMT	$1 \times 2.6$	4800	4750-7400	6
M33-16	1982 Oct 12	MMT Spec. MMT	$1 \times 2.6$	2400	4750-7400	6
M33-4	1982 Oct 22	FLWO 1.5 m Z-machine	7.1	9000	4500-7000	7
M33-1	1982 Oct 24	FLWO 1.5 m Z-machine	$6 \times 12.6$	9000	4500-7000	7

better than 15%, judging again from comparison of results from separate standard stars. Ratios such as  $[\text{O III}] \lambda\lambda 4959, 5007/\text{H}\beta$ ,  $[\text{N II}] \lambda\lambda 6548, 6584/\text{H}\alpha$ , or  $[\text{S II}] \lambda 6717/\lambda 6731$  should be considerably better than this. For example, the  $[\text{S II}]$  lines each contain typically several thousand integrated counts, and because they are close in wavelength, reddening and flux calibration errors should be small. Hence, the  $[\text{S II}]$  line ratios should be accurate to better than 5%. Integration times were chosen so that there were at least 500 total counts in the weakest feature of interest for the abundance analysis, so counting statistics should be small relative to other sources of error. (Any line not meeting this criterion is marked with a colon in Table 2.) For some of the larger SNRs, the spectrograph slits encompassed only a portion of each remnant's spatial extent. This could conceivably cause additional uncer-

tainty if large variations in line intensities from filament to filament are present. Judging from galactic SNRs (cf. Fesen, Blair, and Kirshner 1985), we assume that this effect is small.

The observed integrated line intensities,  $F(\lambda)$ , are shown for each object in Table 2 on a scale where  $\text{H}\beta = 100$ . The absolute fluxes in  $\text{H}\beta$  (through the slits listed for each object in Table 1) are given at the bottom of Table 2. Color excesses are derived from the observed ratios of  $\text{H}\alpha/\text{H}\beta$  and assuming a theoretical  $\text{H}\alpha/\text{H}\beta$  ratio of 3.0, using the technique described by Miller and Mathews (1972). In the absence of other reddening information, this places the remnants in a common reference frame from which they can be compared. The reddening-corrected line intensities,  $I(\lambda)$ , are also given in Table 2.

Comparison of our data with those previously available for the M33 SNRs (Dopita, D'Odorico, and Benvenuti 1980) shows considerable differences in many instances. In particular, the  $\text{H}\alpha/\text{H}\beta$  ratios from Dopita, D'Odorico, and Benvenuti (1980) are systematically larger than ours. We have used Dopita *et al.*'s observed line ratios to derive values of  $E(B-V)$  as described above for our own observations. Figure 2a shows a comparison of the reddening estimates derived from our data relative to those from Dopita, D'Odorico, and Benvenuti (1980) for objects observed by both of us. The figure indicates a severe systematic effect between the two data sets, with Dopita *et al.*'s spectra showing consistently higher reddening. Since our data were obtained and reduced with several different spectrographs and data reduction systems, this effect is not due to our reductions. We suspect a calibration error in Dopita *et al.*'s data as the cause of the difference. [We note that a similar problem has been found in the Herbig-Haro object data from Dopita (1978), which were reduced at Mount Stromlo; subsequent observations (cf. Dopita, Binette, and Schwartz 1982; Hartmann and Raymond 1984) have failed to confirm the high reddening estimates found in that paper. Also, Dopita, Binette, and Schwartz (1982) mention the possibility of a calibration

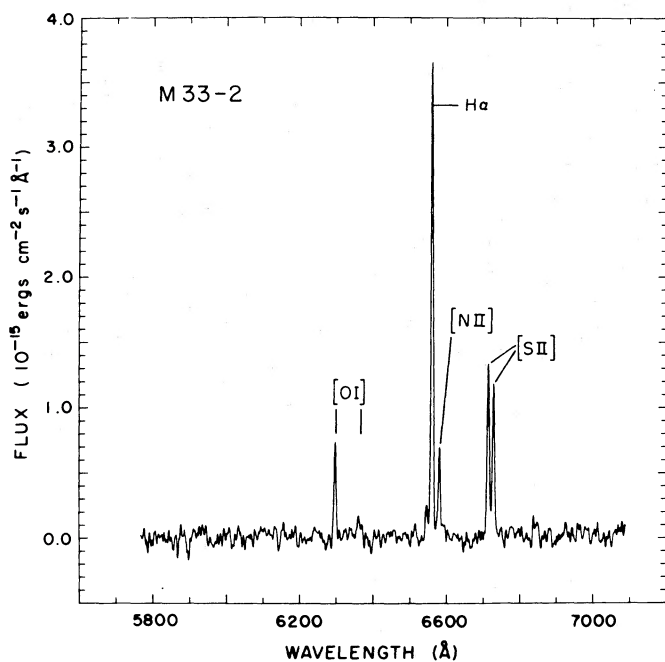


FIG. 1a

FIG. 1.—Representative reduced spectra from the various spectrophotometric systems used to gather optical spectra of M33 SNRs. (a) KPNO 2.1 m/IIDS spectrum of M33-2; (b) McGraw-Hill spectrum of M33-9; (c) MMT spectrum of M33-6 showing full wavelength coverage of Mount Hopkins data; (d) Enlarged portion of M33-6 spectrum from Fig. 1c.

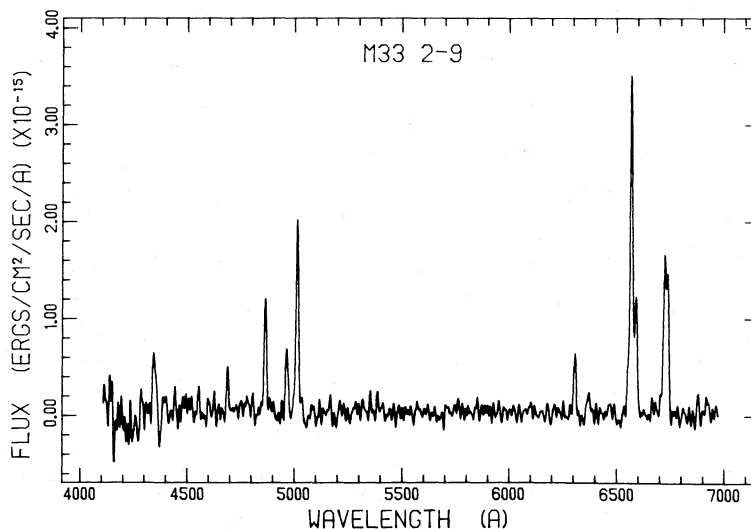


FIG. 1b

error in the earlier data. While the M33 SNR spectra of Dopita, D'Odorico, and Benvenuti (1980) were obtained with the 5 m Hale telescope, they were *reduced* at Mount Stromlo—hence the possible explanation.]

Comparison of line ratios that are not largely dependent on the reddening correction also shows significant differences between the data sets. The density-sensitive ratio of  $[S\ II]\ \lambda 6717/\lambda 6731$  differs substantially (10%–25%) in about half of the 10 objects in common between the samples. In Figure 2b we compare the electron densities as derived from our data and Dopita, D'Odorico, and Benvenuti's (1980) data using the method described in § IV. There is a tendency toward higher densities from our data, with differences of a factor of 2–5 not uncommon. Moreover, these changes systematically occur for the smaller diameter remnants. As indicated in Figure 2c, Dopita, D'Odorico, and Benvenuti's (1980) results showed a large range of densities for the small-diameter remnants and no particular density trend with diameters. The densities derived in this paper show a tendency to decrease with increasing diameter.

The  $[N\ II]/H\alpha$  and  $[S\ II]/H\alpha$  ratios also differ by 15%–35% for about half of the objects. The  $[O\ III]/H\beta$  ratio changes the least, with variations  $\geq 10\%$  for only a few objects. With the exception of the reddening discrepancy, these differences are entirely attributable to the lower resolution ( $\sim 12\ \text{\AA}$ ) and signal-to-noise ratio in the earlier data. Since these ratios are important to the abundance analysis, the abundances derived in the next section deviate significantly from those derived previously for many of the M33 remnants.

### III. ABUNDANCES AND ABUNDANCE GRADIENTS IN M33

#### a) General Comments

The modeling of shock waves has become increasingly sophisticated beginning with the work of Cox (1972a, b). Subsequent workers have incorporated many improvements, including better atomic physics, additional processes such as charge exchange and Auger ionization, and a more consistent accounting of the ionization balance between the preshock and postshock gas (Dopita 1977; Raymond 1979; Shull and

McKee 1979; Butler and Raymond 1980; Dopita *et al.* 1984). These authors have also calculated grids of models to investigate how variations in many parameters can affect the resulting spectrum.

At the same time, improved observations of galactic SNRs such as the Cygnus Loop (Benvenuti, Dopita, and D'Odorico 1980; Raymond *et al.* 1980, 1981; Fesen, Blair, and Kirshner 1982; Hester, Parker, and Dufour 1983) have permitted the shock models to be tested, and some problems and limitations to be identified. The largest discrepancies between the observations and the models occur in the spectra of some individual filaments, where for one of several possible reasons the "steady flow" assumption used in the models apparently breaks down. The spectra of the M33 SNRs include much if not all of the light from each of the SNRs and should be relatively free of effects caused by differences in individual filaments. Each M33 SNR spectrum represents an average of many filaments, weighted by filament brightness. It is a basic assumption in the remainder of this section that it is reasonable to compare these spectra with the shock models.

#### b) Abundance Determinations for M33 SNRs

Of the shock model calculations that are available, those of Dopita and his coworkers (Dopita *et al.* 1984 and references therein) are the most applicable for determining abundances from SNR spectra. The basic conclusion from Dopita *et al.*'s (1984) models is that, for shock velocities  $v_s \geq 100\ \text{km s}^{-1}$ , certain optical line ratios such as  $[O\ III]\ \lambda\lambda 4959, 5007/H\beta$ ,  $[S\ II]\ \lambda 6731/H\alpha$ , and  $[N\ II]\ \lambda\lambda 6548, 6584/H\alpha$  are sensitive primarily to abundance variations and not to shock conditions. The  $[O\ II]\ \lambda 3737$  line, which has been used in previous SNR abundance studies, is found to be a poor abundance diagnostic because it is an important cooling line and saturates very readily. Hence, even though our M33 SNR spectra only go down to  $H\beta$ , this does not affect the abundance determinations.

A serious confusion effect occurs, however, for those objects with small  $[O\ III]/H\beta$  ratios. Unless independent information is available on the shock velocity, a small  $[O\ III]/H\beta$  ratio

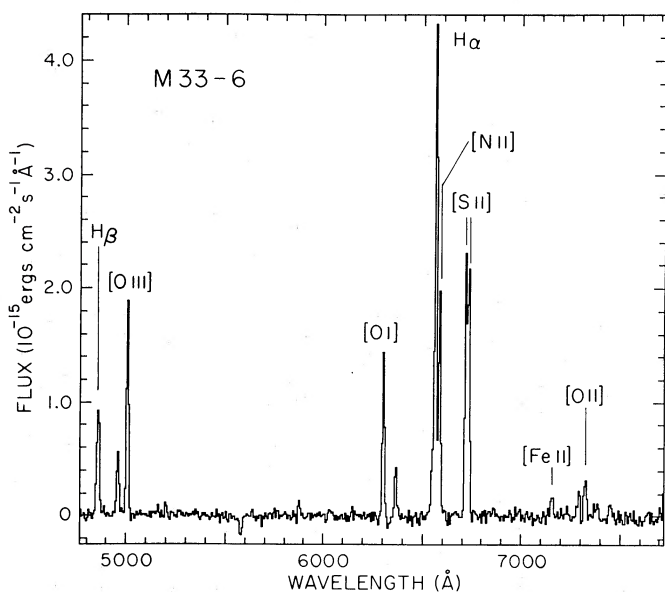


FIG. 1c

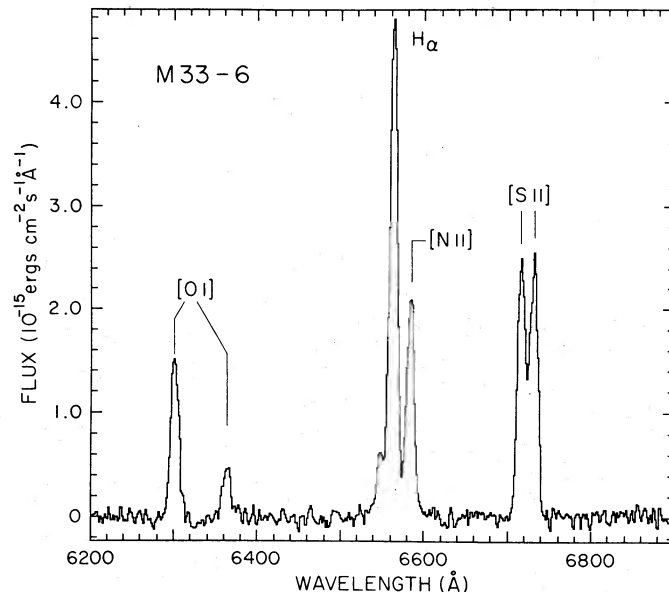


FIG. 1d

TABLE 2  
OBSERVED FLUXES,  $F(\lambda)$ , AND REDDENING CORRECTED FLUXES,  $I(\lambda)$ , RELATIVE TO  $H\beta = 100$

LINE	$\lambda$ (Å)	M33-1		M33-2 <sup>a</sup>		M33-4		M33-5 <sup>a</sup>		M33-6	
		$F(\lambda)$	$I(\lambda)$	$F(\lambda)$	$I(\lambda)$	$F(\lambda)$	$I(\lambda)$	$F(\lambda)$	$I(\lambda)$	$F(\lambda)$	$I(\lambda)$
H $\beta$ .....	4861	100	100	...	...	100	100	...	...	100	100
[O III] .....	4959	39.3	39.1	...	...	37.7	37.3	...	...	48.3	47.9
[O III] .....	5007	114	113	...	...	111	109	...	...	157	155
[Fe II] .....	5156	...	...	...	...	<15	<15	...	...	5.5:	5.4:
[N I] .....	5200	...	...	...	...	<15	<15	...	...	7.8:	7.6:
He I .....	5876	...	...	...	...	<15	<15	...	...	9.8:	9.1:
[O I] .....	6300	50:	46:	58.3	...	40.8	36.5	85.5	...	115	104
[O I] .....	6363	<40	<37	15:	...	15.2	13.5	34.0:	...	35.9	32.3
[N II] .....	6548 <sup>c</sup>	27:	25:	20.1	...	26.0	22.7	35.8	...	52.0	46.3
H $\alpha$ .....	6563	325	300	300	...	340	300	300	...	337	300
[N II] .....	6584	80.0	73.7	60.2	...	77.4	68.1	117	...	156	139
[S II] .....	6716	127	116	118	...	114	99.6	180	...	178	157
[S II] .....	6731	92.0	84.4	106	...	76.2	66.6	137	...	175	154
[Fe II] .....	7155	...	...	...	...	...	...	...	...	15.1:	13.1:
[Fe II] .....	7172	...	...	...	...	...	...	...	...	<5	<4.3
[Ca II] .....	7291	...	...	...	...	...	...	...	...	16.6:	14.3:
[Ca II] + [O II] .....	7320-7230	...	...	...	...	...	...	...	...	32.0:	27.5:
Fe II?, [Ni II] .....	7378	...	...	...	...	...	...	...	...	12:	10:
$F(H\beta)$ (ergs cm <sup>-2</sup> s <sup>-1</sup> ) .....		4.00E - 15		2.68E - 14 <sup>d</sup>		8.07E - 15		9.47E - 15 <sup>d</sup>		1.04E - 14	
$E(B-V)$ .....		0.07		...		0.12		...		0.11	

<sup>a</sup> H $\beta$  not observed; fluxes given relative to H $\alpha$  = 300.

<sup>b</sup> Roughly 40% in broad (SNR) component and 60% in narrow (H II) component.

<sup>c</sup> Assumes  $F(6548) = 0.33 \times F(6584)$ .

<sup>d</sup> Flux in H $\alpha$ .

NOTE.—A colon indicates > 5% error from counting statistics.

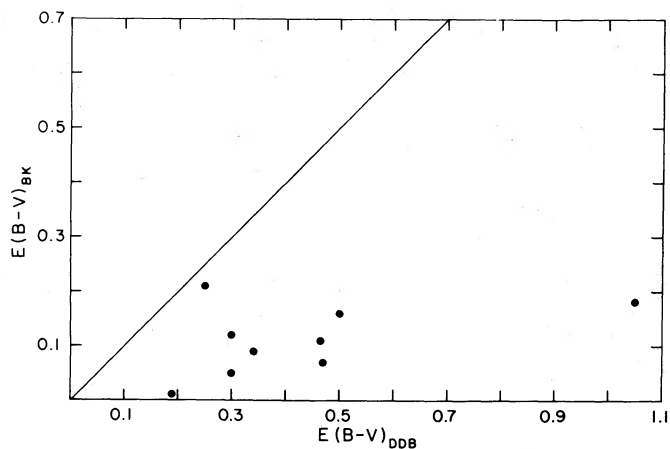


FIG. 2a

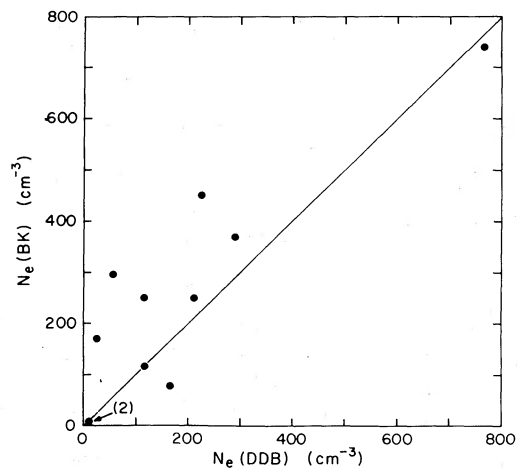


FIG. 2b

FIG. 2.—(a) Comparison of color excesses derived in this paper (*BK*) relative to those from Dopita, D'Odorico, and Benvenuti (1980) (*DDB*). All  $E(B-V)$ 's have been derived from the observed line intensities assuming  $I(H\alpha)/F(H\beta) = 3.0$ . The straight line indicates equality. (b) Comparison of electron densities for M33 SNRs as derived in this paper (*BK*) and by Dopita, D'Odorico, and Benvenuti (1980) (*DDB*). The straight line indicates equality. (c) Comparison of densities derived in this paper (*filled circles*) and Dopita, D'Odorico, and Benvenuti (1980) (*open circles*) as a function of remnant diameter.

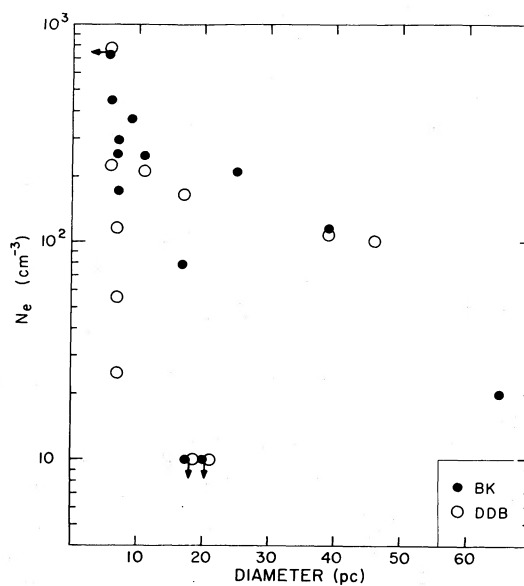


FIG. 2c

TABLE 2—Continued

M33-7		M33-8		M33-9		M33-11		M33-15		M33-16		M33-18	
$F(\lambda)$	$I(\lambda)$	$F(\lambda)$	$I(\lambda)$	$F(\lambda)$	$I(\lambda)$	$F(\lambda)$	$I(\lambda)$	$F(\lambda)$	$I(\lambda)$	$F(\lambda)$	$I(\lambda)$	$F(\lambda)$	$I(\lambda)$
100	100	100	100	100	100	100	100	100	100	100	100	100	100
142	140 <sup>b</sup>	80.5	80.2	58.0	58.0	35.3	35.1	145	113	41.2	40.6	75.8	78.2
446	437 <sup>b</sup>	259	258	171	171	109	108	359	350	123	120	207	205
9.7:	9.3:	4.6:	4.6:	<15	<15	<5	<4.9	<10	<10	<4	<3.8	...	...
<5	<4.8	<4	<4	<15	<15	13.5:	13.3:	<10	<10	5.2:	5.0:	<20	<20
11.1:	9.9:	10.3:	10.0:	<15	<15	9.0	8.6	31.3:	27:	9.1	8.0	25:	23:
75.6	64.7	20.8:	19.9:	50.4	49.8	131	123	44.8:	37:	59.0	49.7	77.7	71.2
24.7	21.0	5.9:	5.6:	17.6:	17.4:	37.6	35.2	<15	<13	15.6:	13.1:	28.8:	26.3:
69.0	57.9	37.8	36.0	37.7	37.2	39.8	37.1	26.8	21.5	26.1	21.5	29.7	26.9
357	300	315	300	304	300	322	300	374	300	364	300	331	300
206	172	114	108	109	108	119	111	81.9	65.4	78.2	64.2	105	95.0
134	111	104	98.6	145	143	202	187	137	108	118	95.7	138	124
159	132	93.1	88.3	123	121	188	174	93.8	74.0	122	99.0	109:	98.0:
15.5:	12.5:	<5	<4.7	...	...	<10	<9.2	<20	<15	<4	<3.1	...	...
17.0:	13.7:	<5	<4.7	...	...	<10	<9.2	<20	<15	<4	<3.1	...	...
<5:	<4:	<5	<4.7	...	...	<8	<7	<15	<11	12:	9.3:	...	...
25.6:	20.4:	<5	<4.7	...	...	10:	9.1:	<15	<11	14:	11:	...	...
64.4	51.0	10:	9.4:	...	...	15:	14:	<15	<11	<8	<6.2	...	...
1.59E - 14		1.26E - 14		1.61E - 14		6.50E - 15		1.31E - 15		5.03E - 15		1.80E - 14	
0.16		0.05		0.01		0.07		0.21		0.18		0.09	

could be due to a low shock velocity ( $v_s < 100 \text{ km s}^{-1}$ ), a low oxygen abundance, or both causes. This point is not addressed fully by Dopita *et al.* (1984) in their reanalysis of the previous M33 and M31 SNR spectra: they implicitly assume that all of the remnants have shock velocities faster than  $\sim 100 \text{ km s}^{-1}$ . While this assumption must be made in order to proceed, this confusion effect can potentially cause a serious problem in the abundance analysis because the abundances of nitrogen and sulfur are determined from the oxygen abundance via the ratios O/N and O/S (cf. Dopita *et al.* 1984, Figs. 10 and 11).

Deciding what constitutes a “small” [O III]/H $\beta$  ratio in the context of the above discussion is somewhat arbitrary, but certainly ratios of [O III]/H $\beta \lesssim 2.0$  could be at least partially due to low  $v_s$ . Inspection of Table 2 (and using [O III]/H $\beta$  ratios from Dopita, D’Odorico, and Benvenuti 1980 for M33-2, M33-5, and M33-14) shows that roughly half of the M33 remnant sample falls into this category. However, the objects with small [O III]/H $\beta$  ratio cannot be dropped from consideration without biasing the sample in the other direction, because then objects with relatively high oxygen abundance would be left in the sample. We will proceed with the abundance determinations assuming the [O III]/H $\beta$  ratio to be an abundance diagnostic only, and will comment on the possible effects of low  $v_s$  in the next section.

Abundance determinations using the models of Dopita *et al.* (1984) are very straightforward. Reddening-corrected line ratios for each object are compared with several diagnostic diagrams (especially those of Dopita *et al.* 1984, Figs. 10 and 11) on which are plotted the results of a grid of models. The [O III]/H $\beta$  and [N II]/H $\alpha$  ratios permit the oxygen abundance and O/N ratio (by number) to be derived while [O III]/H $\beta$  and [S II]  $\lambda 6731$ /H $\beta$  determine O/S. In addition to the reddening-corrected data from Table 2, data for M33-14 and the [O III]/H $\beta$  ratios for M33-2 and M33-5 were taken from Dopita, D’Odorico, and Benvenuti (1980). The derived abundances by number relative to hydrogen for each object are listed in Table 3. Also shown in Table 3 are values of a generalized “metal” abundance parameter for each object which was derived from

the observed line ratios and Figure 18 of Dopita *et al.* (1984), as discussed in that paper.

Average abundances are given at the bottom of Table 3, as are the abundances of the Orion Nebula for comparison (from Peimbert and Torres-Peimbert 1977). The mean relative and absolute abundances of O and N appear to be consistent with those of Orion, while S appears to be lower by roughly a factor of 2.

One object from Table 3 deserves particular mention. Dopita, D’Odorico, and Benvenuti (1980) found systematically higher abundances for the object M33-7 than for the other remnants and attributed this to enhancement from the ejecta of the supernova explosion. This is one of the smallest diameter remnants in the sample ( $D = 6 \text{ pc}$ ), so it might be expected to show signs of enhancement. However, there are several other remnants of comparable or only slightly larger size (M33-16,  $D = 6 \text{ pc}$ ; M33-2,  $D = 7 \text{ pc}$ ; M33-11,  $D = 7 \text{ pc}$ ; M33-6,  $D = 9 \text{ pc}$ ) which do not show obvious signs of enrichment.

The resolution of this discrepancy can be found in higher resolution spectroscopy. Danziger *et al.* (1979) found evidence for a broad component at  $5007 \text{ \AA}$  in their initial spectrum of M33-7 (called M33-1 by them). We have obtained high-resolution ( $\Delta\lambda \approx 0.1 \text{ \AA}$ ) data on M33-7 in the region of H $\alpha$  and [N II], [S II], and [O III]  $\lambda 5007$  using an echelle spectrograph on the MMT. These spectra clearly show broad components with FWHM  $\approx 700 \text{ km s}^{-1}$ , and narrow lines with FWHM  $\approx 75 \text{ km s}^{-1}$ . The H $\alpha$ , [N II], and [S II] lines are dominated by the broad components which contain  $\gtrsim 90\%$  of the integrated flux, but the [O III] line is divided much more evenly, with  $\sim 40\%$  of the flux in the broad component and  $60\%$  in the narrow component. Furthermore, the H $\alpha$ /[N II] and H $\alpha$ /[S II] line ratios in the narrow components look like those of M33 H II regions. Hence, it appears that the narrow lines represent H II region emission, and the broad lines are from an SNR that is probably embedded within the H II region. In lower resolution spectra (cf. Dopita, D’Odorico, and Benvenuti 1980; see also our Table 2) the H II region contamination of the [O III] lines would seriously affect an abundance

TABLE 3  
ABUNDANCES BY NUMBER FOR M33 SUPERNOVA REMNANTS

OBJECT	GALACTOCENTRIC DISTANCE		O/H ( $\times 10^{-4}$ )	N/H ( $\times 10^{-5}$ )	S/H ( $\times 10^{-6}$ )	log $A^b$
	R (kpc)	$R/R_0^a$				
M33-1	4.37	0.76	2.3	2.2	4.1	-3.77
M33-2	4.16	0.72	2.4	1.9	4.9	-3.75
M33-4	3.72	0.64	2.1	2.0	3.2	-3.80
M33-5	3.05	0.53	2.9	3.8	7.2	-3.55
M33-6	2.02	0.35	3.1	4.6	8.6	-3.44
M33-7	1.58	0.27	3.5	5.9	8.0	-3.42
M33-8	0.78	0.14	5.4	4.1	7.0	-3.52
M33-9	1.55	0.27	3.5	3.7	7.1	-3.55
M33-11	1.34	0.23	2.1	3.3	9.4	-3.57
M33-14	2.87	0.50	5.1	3.1	7.1	-3.60
M33-15	2.89	0.50	8.5	4.3	9.4	-3.63
M33-16	2.98	0.52	2.4	2.1	4.7	-3.77
M33-18	3.43	0.59	4.4	3.3	6.7	-3.60
Averages	...	...	$3.7 \pm 1.9$	$3.2 \pm 1.0$	$6.6 \pm 2.0$	...
Orion <sup>c</sup>	...	...	3.3	3.7	15	...

<sup>a</sup>  $R_0 = 5.77$  kpc; see text.

<sup>b</sup>  $A$  = generalized "metal" abundance calculated as described by Dopita *et al.* 1984.

<sup>c</sup> From Peimbert and Torres-Peimbert 1977.

analysis. We have derived the abundances shown for M33-7 in Table 3 after correcting the line strengths listed in Table 2 for the effects of the H II region contamination. These abundances do not appear to be significantly enhanced relative to the other SNRs, so M33-7 will be included in the abundance gradient analysis. A more complete analysis of this interesting object, including an ultraviolet spectrum, will be published separately (Blair *et al.* 1985). However, it is mentioned here to establish the seriousness of possible H II region contamination on SNR abundance analyses.

c) *Abundance Gradients for M33 SNRs, and Comparison with H II Region Results*

Column (2) of Table 3 lists the galactocentric distances  $R$  in kpc for each of the SNRs, assuming a distance of 720 kpc, an inclination of  $33^\circ$ , and a major-axis position angle of  $20^\circ$  (Searle 1971). Also shown are values of  $R$  scaled relative to  $R_0$ , the isophotal radius where the galaxy surface brightness becomes 25 mag arcsec<sup>-2</sup> (corrected to face-on and corrected for galactic extinction), taken from de Vaucouleurs, de Vaucouleurs, and Corwin (1976); for M33,  $R_0 = 5.77$  kpc for the distance assumed above. The relative merits of these two methods of scaling gradients will be discussed below.

Figures 3a, 3b, and 3c show the M33 abundance gradient results for O, N and S, respectively. The filled circles are the M33 SNRs, and the solid line in each case is a least squares fit to the SNR data. The slopes of these lines are the SNR abundance gradients, which are summarized in Table 4 and parameterized both in terms of absolute distance from the galaxy's center and in terms of the isophotal radius  $R_0$ .

The open circles shown in Figures 3a, 3b, and 3c are the H II region abundance determinations of Kwitter and Aller (1981). Roughly half of these 11 H II regions have some direct temperature information from spectroscopic line ratios, and in these cases abundances have been derived in a straightforward manner. The abundances in the remaining cases depend on a combined method of H II region model fitting and empirical temperature indicators. The merits and uncertainties of this

technique have been discussed at length by many authors (Alloin *et al.* 1979, Pagel, Edmunds, and Smith 1980; Pagel and Edmunds 1981; Stasinska *et al.* 1981; Blair, Kirshner, and Chevalier 1982) and will not be discussed here. Suffice it to say that for the H II regions with empirical temperature determinations, the abundances are more uncertain (roughly 0.3 dex). The two points with error bars are H II regions for which more than one

TABLE 4  
M33 AND M31 ABUNDANCE GRADIENT SUMMARY

Element	$\frac{d(\log Z/H)}{dR}$ (dex kpc <sup>-1</sup> )	$\frac{d(\log Z/H)}{d(R/R_0)}$ (dex)	Mean Variation from Least Squares Line (dex)
M33 SNRs			
O	-0.035	-0.199	0.134
N	-0.089	-0.512	0.086
S	-0.092	-0.541	0.096
$A^a$	-0.083	-0.508	0.067
M33 H II Regions <sup>b</sup>			
O	-0.099	-0.566	0.095
N	-0.108	-0.624	0.074
S	-0.037	-0.211	0.134
M31 SNRs <sup>c</sup>			
O	+0.004	+0.056	0.139
N	-0.040	-0.591	0.108
S	-0.023	-0.335	0.116
$A^a$	-0.029	-0.579	0.104
M31 H II Regions <sup>c</sup>			
O	-0.030	-0.446	0.112
N	-0.045	-0.673	0.100
S	-0.031	-0.469	0.136

<sup>a</sup>  $A$  = generalized "metal" abundance as described by Dopita *et al.* 1984.

<sup>b</sup> Using data from Kwitter and Aller 1981.

<sup>c</sup> From Blair, Kirshner, and Chevalier 1982.

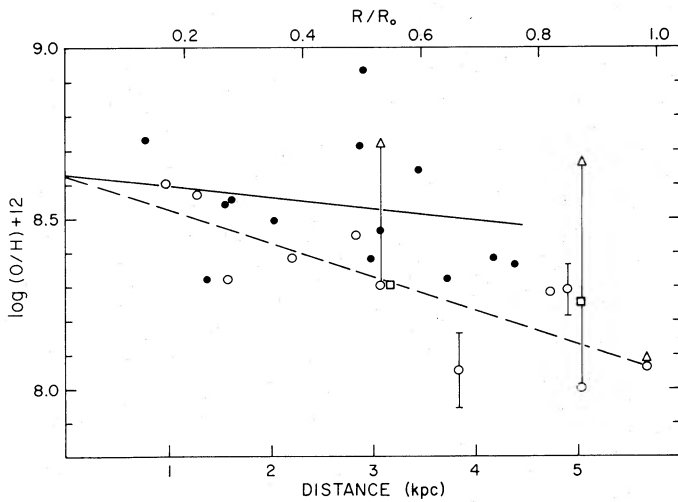


FIG. 3a

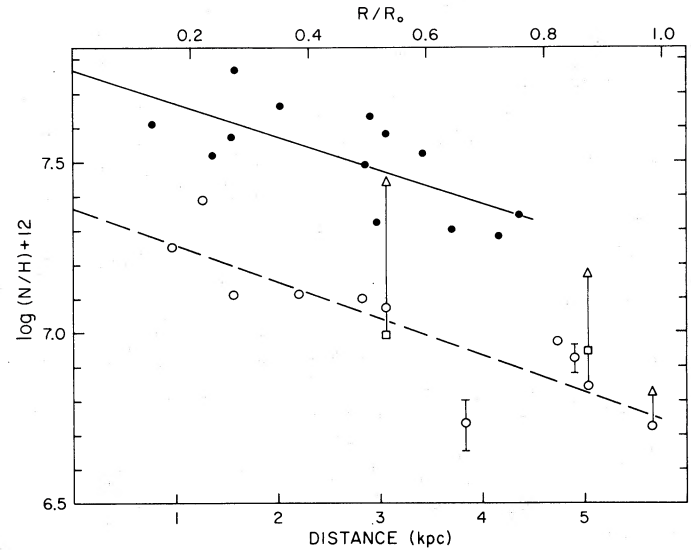


FIG. 3b

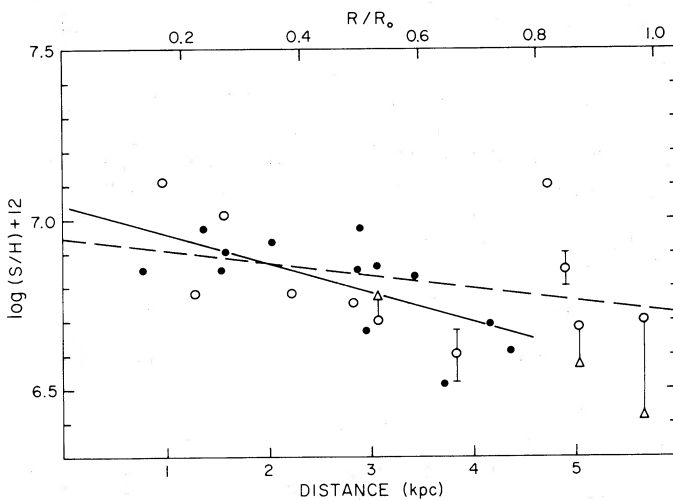


FIG. 3c

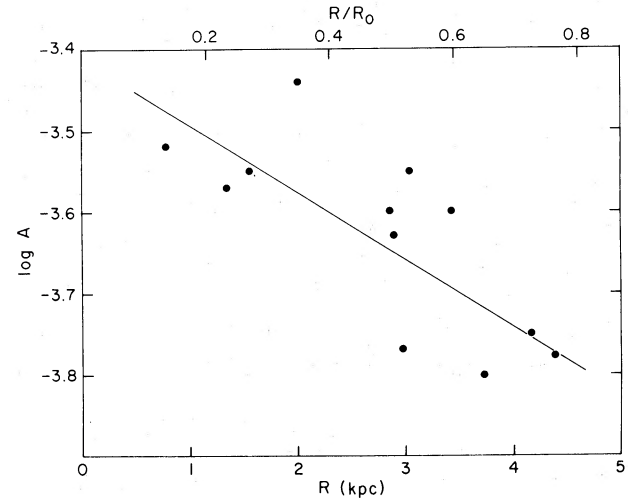


FIG. 3d

FIG. 3.—(a) M33 O abundance gradients from SNRs (*filled circles*) and H II regions (*open symbols*). Open circles are data from Kwitter and Aller (1981), open squares are from Dufour, Schiffer, and Shields (1984), and open triangles are from Smith (1975). The solid lines and dashed lines are least squares fits to the SNR and Kwitter and Aller H II region data, respectively.  $R_0$  is an isophotal radius, as described in the text. (b) Same as Fig. 3a, but for N. (c) Same as Fig. 3a, but for S. (d) Dopita *et al.*'s (1984) "metal" abundance parameter,  $\log A$ , as a function of galactocentric distance for the M33 SNRs. The line is a least squares fit.

position was observed, and the error bars indicate the range of derived abundances. The dashed lines are least squares fits to the Kwitter and Aller (1981) H II region abundances, and the slopes of these lines are listed in Table 4 for comparison with the SNR results.

Dufour, Schiffer, and Shields (1984) have derived C, N, and O abundances for two M33 H II regions observed by Kwitter and Aller (1981) (NGC 604 and NGC 588). The results for O and N are shown in Figures 3a and 3b as open squares, and the agreement with Kwitter and Aller is acceptable. Smith (1975) observed three of Kwitter and Aller's H II regions (NGC 604, NGC 588, and IC 132), and his results are shown as open triangles in Figures 3a, 3b, and 3c. His O and N abundances are systematically higher than Kwitter and Aller's for NGC 604 and NGC 588 ( $\sim 0.4$  dex), although agreement is found for IC 132. These differences are due largely to the different temperatures derived from the spectroscopic data ( $\Delta T_e \gtrsim 1500$  K)

as well as to the inclusion of charge-exchange reactions in the more recent analysis.

Figure 3a indicates that a well-defined oxygen abundance gradient is present in the H II region data. As mentioned by Kwitter and Aller (1981), the temperatures in the inner H II regions may be even lower than they assumed, which would mean that the O abundances could be larger than shown. Hence, the gradient may be even steeper than is implied by the least squares fit. In contrast, there is more scatter in the SNR data, and while the least squares line does have a negative slope, it is not significant in comparison with the uncertainties.

The large scatter and lack of a clear O gradient from the M33 SNRs are attributable to two causes. One is the possible confusion from remnants with low shock velocity, as was discussed earlier. The most likely example is M33-11, which has the lowest O abundance in the sample even though it is relatively near the center of M33 ( $R = 1.34$  kpc). The  $[\text{O III}]/\text{H}\beta$

ratio for this object is 1.43, which places it in the “suspect” range. However, no other velocity information is available for this remnant, so the interpretation remains ambiguous. The other problem is possible contamination from nearby photoionized regions. The M33 H II regions show a wide range of excitation, with  $[\text{O III}]/\text{H}\beta$  generally increasing outward from the center. Since  $[\text{O III}]$  can be quite strong in photoionized gas, one would expect the  $[\text{O III}]/\text{H}\beta$  ratio to be most seriously affected, as was the case for SNR M33-7 discussed earlier. The three objects near  $R \approx 3$  kpc that are substantially above the O least squares line for SNRs are M33-14, M33-15, and M33-18. Inspection of the regions around these remnants on image-tube photographs of M33 obtained by us with the 1.3 m telescope at McGraw-Hill Observatory (see also finder charts in D’Odorico, Dopita, and Benvenuti 1980) shows that H II region contamination is not only possible but probable for M33-14 and M33-15, and possible for M33-18. For comparison, the H II region MA 3 observed by Kwitter and Aller (1981) is about 2.8 kpc from the center of the galaxy, and has  $[\text{O III}]/\text{H}\beta = 5.7$ . Within these uncertainties, the absolute O abundances as derived from SNRs and H II regions are in reasonable agreement, and the O abundance gradient from H II regions is probably real.

The situation for N, as shown in Figure 3b, is very interesting. The N abundance gradients as derived from SNRs and H II regions are identical within the accuracy of their determination, but the SNR abundances are systematically higher by about 0.4 dex. This difference is perplexing because N is not a strong coolant in either shock-heated or photoionized gas, and previous investigations (Dopita, D’Odorico, and Benvenuti 1980; Blair, Kirshner, and Chevalier 1982) indicated good agreement between SNRs and H II regions in terms both of N gradients and of absolute abundances. However, these studies used Dopita’s models in their earlier form (Dopita 1977), and the discrepancy occurs when the newer models (Dopita *et al.* 1984) are used.

To check Dopita *et al.*’s (1984) models, we have used an updated version of the Raymond (1979) shock code to calculate several test cases with reasonable shock conditions ( $v_s = 90$  and  $120 \text{ km s}^{-1}$ ,  $n_0 = 2\text{--}5 \text{ cm}^{-3}$ ) and “M33-like” abundances. While these models are preliminary, they do indicate N abundances of roughly  $12 + \log \text{N}/\text{H} = 7.55$ , very much in line with the results of Dopita *et al.*’s (1984) models.

If N is really more abundant in the SNRs than in the H II regions, it is difficult to conceive of a viable mechanism of enrichment. N is traditionally thought to be one of the least depleted elements in interstellar gas (cf. Seab and Shull 1983), and while grains are thought to be at least partially destroyed in SNR shocks (Draine and Salpeter 1979), there is no reason to expect N to be *selectively* enhanced. Also, with the range of remnant diameters included in the M33 sample (6–65 pc), enhancement by supernova ejecta cannot account for the difference. This discrepancy is also present between SNRs and H II regions in M31 (see below), our Galaxy (Fesen, Blair, and Kirshner 1985), and the LMC (Evans and Dopita 1985). The last reference indicates that the problem may be associated with the H II region analysis.

The S abundances from SNRs and H II regions in M33 agree about as well as could be expected (see Fig. 3c), given the substantial uncertainties in determining S abundances for H II regions when the  $[\text{S III}] \lambda\lambda 9069, 9532$  lines have not been observed (Hawley and Grandi 1977). Interference-filter photographs of galactic SNRs (cf. Fesen, Blair, and Kirshner 1982)

show that H $\alpha$  and  $[\text{S II}]$  emission are very nearly coextensive, so the SNR results may be somewhat more reliable in this case. The S gradient indicated by the SNR data is very similar to that found for N and to the O gradient from H II regions.

M31 is the only other external galaxy for which an effective comparison of SNR and H II region abundance gradients can currently be made. We have reanalyzed our M31 SNR data (Blair, Kirshner, and Chevalier 1982) using Dopita *et al.*’s (1984) new shock models, and show the results in Figures 4a, 4b, and 4c and Table 4, along with M31 H II region results. The comparison in M31 is very analogous to that in M33. The use of the new models has partially removed the discrepancy between the H II region and SNR results for O (see Blair, Kirshner, and Chevalier 1982, Fig. 7b), although the SNRs still do not show evidence for an abundance gradient (see Fig. 4a). The results for N (Fig. 4b) show the same dichotomy as found in M33: the gradients from SNRs and H II regions are very similar, but the SNR abundances are higher by roughly 0.3 dex. The S results (Fig. 4c) are quite similar and indicate that a moderate S abundance gradient is present in M31.

Dopita *et al.* (1984) claim that the M31 SNRs do not show an O abundance gradient like that found for M31 H II regions because of a saturation effect in the SNR models at high abundances. According to Dopita *et al.*, this occurs at  $Z(\text{O}) \approx 2 \times 10^{-4}$ , or  $\log \text{O}/\text{H} + 12 \approx 9.3$ . Using the H II regions in Figure 4a as an indication, the inner regions of M31 have an O abundance of roughly  $\log \text{O}/\text{H} + 12 \lesssim 9.2$  (see also Pagel and Edmunds 1981), so this saturation effect may not be negligible, but neither should it be dominant. Since a similar situation occurs in M33 where the mean O abundance is  $\sim 0.5$  dex lower, we believe that the problem of contamination of the SNR sample by low-velocity shocks and photoionized regions may also be important in M31.

Dopita *et al.* (1984) use their model predictions to define a general metal abundance parameter,  $\log A$ , that gives an estimate of the “metallicity” of an object to an accuracy of  $\sim 0.2$  dex. We have used the line ratios obtained from Table 2 with Figure 18 from Dopita *et al.* (1984) to determine  $\log A$  for each of the M33 remnants. The results are shown in Figure 3d and Table 4 and can be directly compared to Dopita *et al.*’s (1984) Figure 20. An “abundance” gradient is clearly present, with a slope very similar to the N gradients found above for M33 and slightly reduced scatter from the individual N and S results. Note that the “stair-step” effect seen in  $\log A$  for M33 by Dopita *et al.* (1984) is much less apparent with our improved observations. Dopita *et al.* (1984) show the gradient in  $\log A$  for the M31 SNRs in their Figure 19.

The comparison of abundance gradients between one spiral galaxy and another is complicated by many factors (cf. discussion in Blair, Kirshner, and Chevalier 1982). One of the most fundamental problems has been determining the most physically meaningful method for making such comparisons. Dufour *et al.* (1980) preferred the use of linear radius (in kpc) to compare five luminous spirals. Many authors have used the isophotal radius,  $R_0$ , to scale galaxies relative to one another, although the physical reason why this radius is meaningful has never been identified. Whitmore (1984) has recently performed a principal-components analysis for a sample of spiral galaxies and finds spirals to be dominated by two dimensions. The “scale” dimension is closely associated with  $R_0$ , and may give credence to its use in galaxy comparisons.

Table 7 of Blair, Kirshner, and Chevalier (1982) shows a compendium of abundance gradient results from several spiral

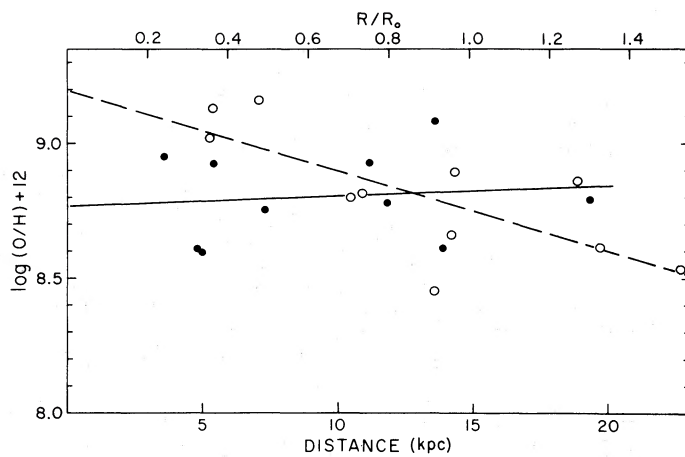


FIG. 4a

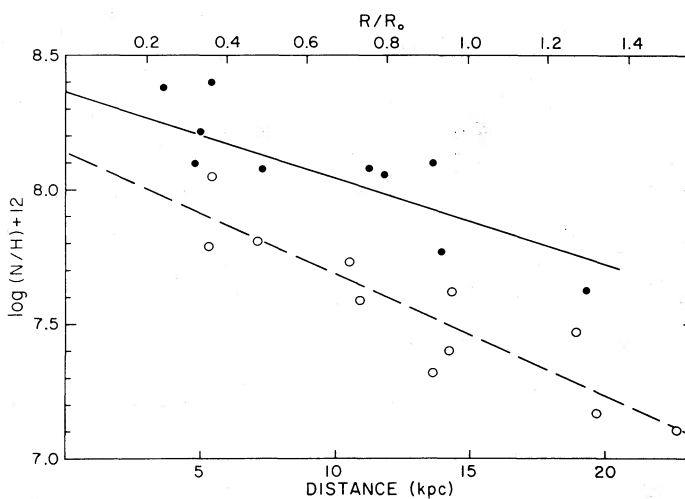


FIG. 4b

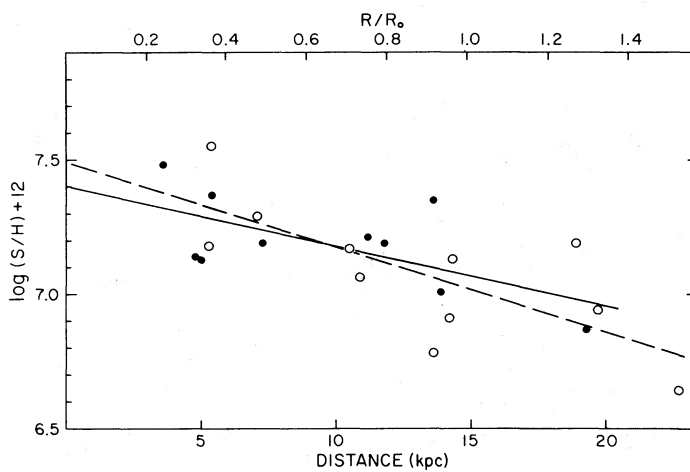


FIG. 4c

FIG. 4.—(a) M31 O abundance gradient for SNRs (filled circles) and H II regions (open circles) using data from Blair, Kirshner, and Chevalier (1982). The SNR data have been reanalyzed using the shock models of Dopita *et al.* (1984). (b) Same as Fig. 4a, but for N. (c) Same as Fig. 4a, but for S.

galaxies. Since M33 is classified as SAcd II–III, one might expect it to be most similar to NGC 300 (Pagel *et al.* 1979, SAd III–IV). In absolute units, the NGC 300 gradients from five H II regions are  $d(\log \text{O}/\text{H})/dR = -0.09 \text{ dex kpc}^{-1}$  and  $d(\log \text{N}/\text{H})/d(R/R_0) = -0.11 \text{ dex}$ , nearly identical with the M33 results shown in Table 4. The mean O and N abundances for H II regions in the two galaxies are also quite similar (O may be more abundant in NGC 300 by  $\sim 0.25 \text{ dex}$ ). This accentuates the discrepancy found for the N abundance between M33 SNRs and H II regions. The gradients in  $R_0$  units are slightly steeper in M33 because  $R_0$  is slightly larger than in NGC 300 ( $R_0 = 5.35 \text{ kpc}$ ).

In a similar manner, one might expect the abundance gradients in M31 and our Galaxy to agree, since both are classified SABbc II. Talent and Dufour (1979) and Shaver *et al.* (1983) give H II region results for our Galaxy, and SNR gradients have recently been derived by Binette *et al.* (1983) and Fesen, Blair, and Kirshner (1985). The N gradient from H II regions and SNRs in our Galaxy is very similar,  $d(\log \text{N}/\text{H})/dR = -0.09 \text{ dex kpc}^{-1}$ , although the mean SNR abundance of N is about 0.6 dex higher (i.e., similar to the situation for M33 and M31). Comparison with Table 4 indicates that this is about a factor of 2 steeper than the N gradient in M31, but about equal to that of M33. The situation is nearly the same for O: Shaver *et al.* (1983) give  $d(\log \text{O}/\text{H})/dR = -0.07 \text{ dex kpc}^{-1}$  for galactic H II regions, which is about a factor of 2 steeper than for M31, and marginally shallower than the O gradient in M33.

A value of  $R_0 = 11.5 \text{ kpc}$  has been derived for our Galaxy, although it is based on a model of how the Milky Way would appear when viewed from outside (de Vaucouleurs and Pence 1978). Using this value, the O and N gradients in  $R_0$  units become  $-0.8$  and  $-1.0 \pm 0.2 \text{ dex}$ , respectively, which are significantly steeper than found for M31 or M33 (see Table 4). We note that the galactic  $R_0$  would have to be lowered to roughly 7 kpc to make the Milky Way and M31 gradients agree in  $R_0$  units, but that an  $R_0$  this low is probably outside the range of uncertainty in the de Vaucouleurs and Pence (1978) model. Hence, it appears there are real differences between the abundance gradients in M31 and our Galaxy in either linear or  $R_0$  units.

#### IV. EVOLUTIONARY CONSIDERATIONS

##### a) Densities and Initial Energies

In order to explain the coexistence of X-ray and optical emission from SNRs, the following picture has been developed (cf. McKee and Cowie 1975). We assume that the interstellar medium (ISM) consists of many small density enhancements (clouds) embedded within a substrate of very low density material (the intercloud regions). The blast wave from a supernova propagates adiabatically through this medium, heating the intercloud regions to X-ray temperatures and driving slower shocks into the clouds; it is the cooling behind these cloud shocks that produces filaments. Within this picture, it is expected that rough pressure equilibrium should be maintained between the cloud and intercloud regions. If the SNR diameter is known and the pressure can be measured, the supernova energy,  $E_0$ , can be obtained from

$$E_0 = 2.5 \times 10^{45} n_0 V_b^2 [D(\text{pc})]^3 \text{ ergs}, \quad (1a)$$

$$= 2.5 \times 10^{45} (\beta')^{-1} n_c v_c^2 [D(\text{pc})]^3 \text{ ergs} \quad (1b)$$

(McKee and Cowie 1975, eqs. [25] and [26]), where  $n_0$  is the

preshock intercloud density,  $n_c$  is the preshock cloud density,  $V_b$  and  $v_c$  are the intercloud and cloud blast wave velocities in units of  $100 \text{ km s}^{-1}$ ,  $D(\text{pc})$  is the SNR diameter in pc, and  $\beta'$  is the ratio of pressures in the cloud and intercloud regions. (In the discussion below, we assume  $\beta' = 1$ .)

Shock model calculations demonstrate that  $\text{S}^+$  is nearly always formed in the region of the cooling and recombination zone near  $T \approx 10^4 \text{ K}$ . Since the ratio  $[\text{S II}] \lambda 6717/\lambda 6731$  is sensitive to density, accurate measurement of this ratio provides an optical measurement of the gas pressure (see discussion in Blair, Kirshner, and Chevalier 1981). Quantitatively, we find

$$N(\text{S II}) = 45 n_c v_c^2 \text{ cm}^{-3} \quad (2)$$

(cf. Dopita 1977, 1979), so that an optically determined supernova energy estimate can be obtained from

$$E_0(\text{optical}) = 5.5 \times 10^{43} N(\text{S II}) [D(\text{pc})]^3 \text{ ergs}. \quad (3)$$

Blair, Kirshner, and Chevalier (1981) found that the energies of the M31 SNRs derived in this manner did not scatter around some mean value as might be expected, but rather increased as a function of remnant diameter. The same result was also indicated for remnants in the LMC, M33 (using the data of Dopita, D'Odorico, and Benvenuti 1980), and our own Galaxy. Since the  $[\text{S II}]$  lines only measure the thermal component of the pressure, the change of  $E_0$  with diameter can be interpreted as an evolution of the thermal energy component with age. The M33 SNR sample contains smaller diameter remnants and a larger range of remnant diameters than the other samples, so it is particularly useful for studying this effect. Below we will use our improved observations in M33 to reinvestigate this  $E_0$ - $D$  relation.

The heart of this technique is an accurate determination of the  $[\text{S II}] \lambda 6717/\lambda 6731$  line ratio, which allows the electron density (and hence the pressure and  $E_0$ ) to be derived. The relative intensities of the  $[\text{S II}]$  lines have been derived for all of the Mount Hopkins spectra using a Gaussian fitting routine written by Neal Burnham at the Center for Astrophysics. The fitting is done by assuming a fixed separation of the lines ( $= 14.4 \text{ \AA}$ ) and requiring that the Gaussian widths of the two lines be the same. An example of one of the fits is shown in Figure 5. The relative line intensities for the KPNO and McGraw-Hill spectra come directly from the measuring programs used in the reduction, and the data for M33-14 are again taken from Dopita, D'Odorico, and Benvenuti (1980).

The density sensitivity of the  $[\text{S II}]$  lines has been an effective spectral diagnostic in H II regions, planetary nebulae, and SNRs for many years. Improved atomic parameters for  $\text{S}^+$  have become available over the last five or six years, but many people still use the older data listed by Osterbrock (1974), causing confusion in the literature. We have performed a five-level atom calculation for  $\text{S}^+$  using the collisional cross sections of Pradhan (1978) and the new transition probabilities of Mendoza and Zeppen (1982). The code is a modified subroutine from John Raymond's shock model code and has been extensively tested. The resulting relation between the  $\lambda 6717/\lambda 6731$  ratio and  $N_e$  is shown in Figure 6. Densities read from Figure 6 are appropriate for  $T = 10^4 \text{ K}$ , but can be scaled to other temperatures by multiplying by  $(10^4/T_e)^{0.5}$ .

The resulting densities for the M33 SNRs are shown in Table 5, along with optically determined radii (from Dopita, D'Odorico, and Benvenuti 1980) and values of  $E_0$  calculated from equation (3). One additional M33 SNR with a measured

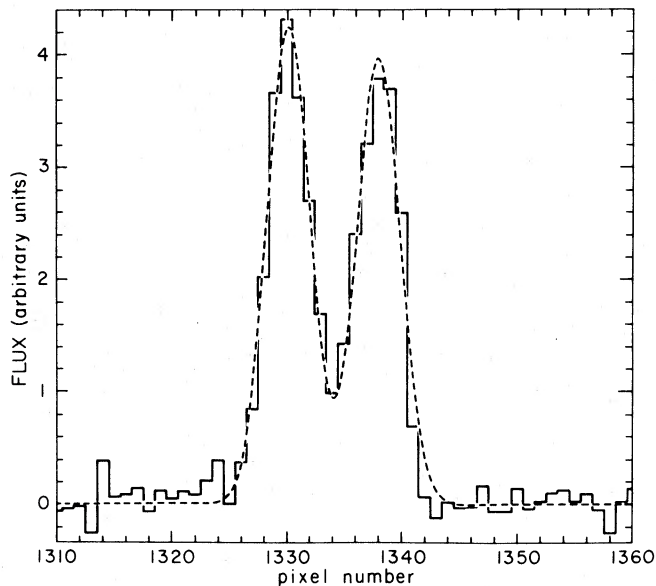


FIG. 5.—Gaussian fit for the [S II]  $\lambda\lambda 6717, 6731$ , lines (smooth curve) relative to the observed line intensities (histogram curve) for M33-11. Gaussian fits such as this were used to derive the  $\lambda 6717/\lambda 6731$  ratios for the Mount Hopkins spectra.

[S II] ratio (S-13, from Sabbadin 1979) is also included in Table 5, although it is less accurate than our data. Figure 7 shows a plot of  $E_0$  against remnant diameter, and it is clear that the M33 SNR sample shows a tight correlation similar to that which was seen for the M31 SNRs. Also shown in Figure 7 are lines of constant density, and the tendency of smaller diameter remnants to have somewhat higher densities (cf. Fig. 2c) is apparent. The maximum values of  $E_0$  near  $10^{51}$  ergs are consistent with the estimated kinetic energy of extragalactic supernova explosions.

The correlation seen in Figure 7 indicates an evolution of the thermal energy component of the M33 SNRs with diameter, and hence with age. The question remains what energy component is being thermalized, as both magnetic pressure (Blair, Kirshner, and Chevalier 1981) and kinetic energy (Long 1983)

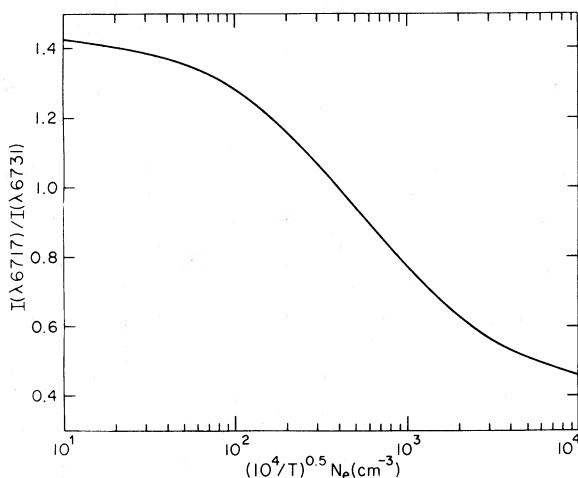


FIG. 6.—The [S II]  $\lambda 6717/\lambda 6731$  ratio as a function of electron density, as derived from a five-level atom calculation and the latest atomic parameters (see text).

TABLE 5  
RADII, DENSITIES, AND ENERGIES<sup>a</sup> OF M33 SNRS

Object	Radius (pc)	$N_e$ (S II) ( $\text{cm}^{-3}$ )	$E_0$ ( $10^{50}$ ergs)
M33-1	32.5	40	6.1
M33-2	3.5	250	0.048
M33-4	9.0	< 10	< 0.032
M33-5	8.5	78	0.21
M33-6	4.5	370	0.15
M33-7	$\approx 3.0$	740	< 0.090
M33-8	5.5	250	0.19
M33-9	3.5	170	0.032
M33-11	3.5	295	0.056
M33-14	23.0	100	5.4
M33-15	10.0	< 10	< 0.044
M33-16	3.0	450	0.054
M33-18	19.5	115	3.8
S-13 <sup>b</sup>	12.4	210:	1.8:

<sup>a</sup> Energy determinations assume  $\beta' = 1.0$ .

<sup>b</sup> From the photographic spectrum of Sabbadin 1979; colon indicates larger uncertainty in this value.

have been suggested. A potential method for answering this question would be to compare to values of  $E_0$  derived from the intercloud gas (i.e., from the X-ray data); the densities are too low and temperatures too high in the intercloud region for the magnetic pressure argument to be viable. If the transfer of kinetic energy to thermal energy is correct, the plot of  $E_0$ (X-ray) against  $D$  should show a correlation similar to that seen for the optical, while if the magnetic pressure argument is correct, no such correlation should be present in the X-ray data.

It is unfortunate that the X-ray surveys of M33 and M31 failed to detect most of the optical SNRs, so this comparison cannot be made with these SNR samples. The LMC remnant sample (Mathewson *et al.* 1983 and references therein) is the most consistent set of X-ray data, but the quality of published optical spectroscopic data for LMC remnants is generally poor. Also, the derivation of  $E_0$  from X-ray data depends on a

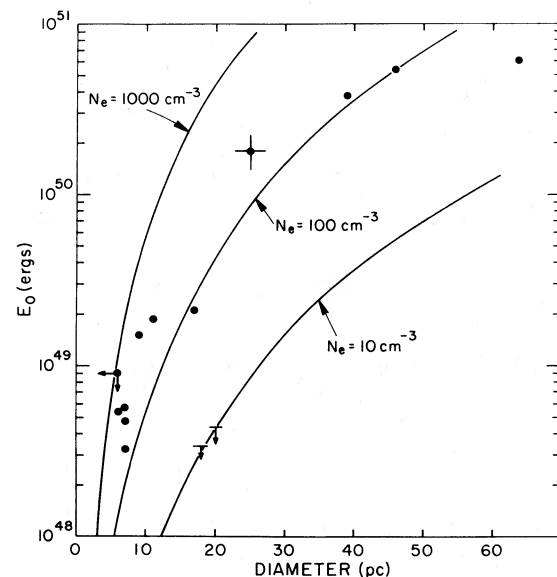


FIG. 7.—Initial energy for M33 SNRs calculated using eq. (3). Solid lines are curves of constant density. The “cross” is from a photographic spectrum of an additional M33 SNR by Sabbadin (1979).

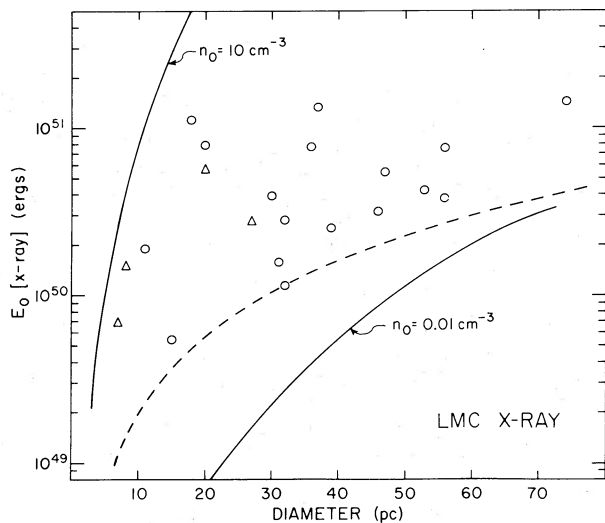


FIG. 8a

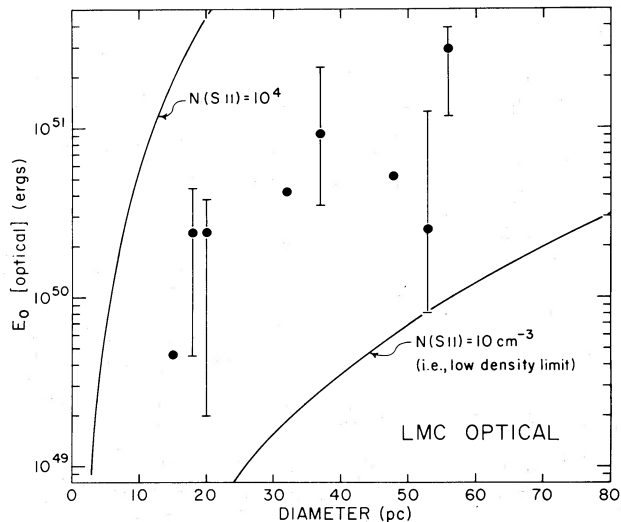


FIG. 8b

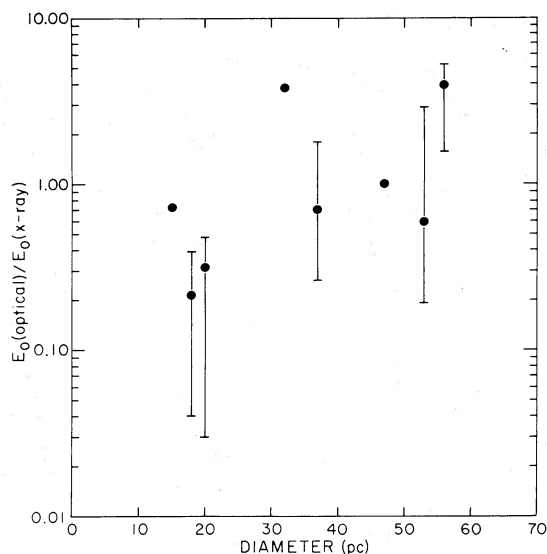


FIG. 8c

FIG. 8.—(a) The  $E_0$ - $D$  relation for LMC X-ray SNRs. The triangles are four Balmer-line remnants, and the dashed line is a lower limit imposed by the X-ray detection threshold of the *Einstein* survey of the LMC. Lines of constant preshock density are also indicated. (b) The  $E_0$ - $D$  relation for eight optical LMC remnants for comparison with Fig. 8a. Lines of constant [S II] density are shown. (c) Comparison of optical and X-ray determinations of  $E_0$  for eight LMC remnants.

number of parameters that are poorly observed or must be assumed. Nonetheless, because of the important ramifications, we proceed with this comparison for the LMC remnants.

Long (1983) and Long, Helfand, and Grabelsky (1981) describe how the X-ray luminosity,  $L_x$ , as derived from the *Einstein* Observatory survey of the LMC, can be used to calculate  $n_0$ , viz.,

$$n_0 = 1.38 f^{1/2} L_x^{1/2} \epsilon^{1/2} [D(\text{cm})]^{-3/2} \text{ cm}^{-3}, \quad (4)$$

where  $f$  is the X-ray filling factor,  $L_x$  is the 0.15–4.5 keV X-ray luminosity in ergs,  $\epsilon$  is the X-ray emissivity ( $\text{ergs cm}^{-3} \text{ s}^{-1}$ ), and  $D$  is the SNR diameter in cm. Implicit in the derivation of  $L_x$  is the assumption of an X-ray temperature and a correction for absorption. Following Long (1983), we have assumed  $T_x =$

$5 \times 10^6 \text{ K}$ ,  $f = 0.25$  (appropriate for a filled shell), and  $\epsilon = 3 \times 10^{-23}$  (for solar abundances from Raymond and Smith 1977). By assuming a strong shock (i.e.,  $n_x = 4n_0$ ), and since  $T_x$  is related to  $V_b$  by

$$T_x = 1.45 \times 10^5 V_b^2 \quad (5)$$

(cf. Fesen and Kirshner 1980), the pressure in the X-ray gas can be derived and equation (1a) becomes

$$E_0(\text{X-ray}) = 8.6 \times 10^{46} n_0 [D(\text{pc})]^3. \quad (6)$$

Figure 8a shows the results of applying equation (6) to the LMC remnants listed by Mathewson *et al.* (1983). We have excluded the two oxygen-rich remnants N132D and 0540–69.3, since the emissivity may be much higher in these objects than we have assumed. We have also excluded the two Crab Nebula-like N103B and N157B, since their X-ray emission may be generated by a different mechanism. This leaves a sample of 21 X-ray SNRs for the LMC.

As reported by Long (1983), there does appear to be a trend in  $E_0(\text{X-ray})$  with  $D$ , although the trend is not well defined. However, this apparent trend may be the result of a selection effect. The *Einstein* survey had a luminosity limit of  $\sim 10^{35} \text{ ergs s}^{-1}$ , and since  $L_x$  depends on  $D$  and  $n_0$  (cf. eq. [4]), part of the  $E_0$ - $D$  plane is discriminated against. The dashed line in Figure 8a indicates the lower limit of the region accessible by the *Einstein* survey, and it is clear that much of the apparent trend is due to the luminosity limit of the survey. The X-ray observations are consistent with an intrinsic spread of roughly 1.5 orders of magnitude in  $E_0$  and about 2.5 orders of magnitude in  $n_0$ .

Optical determinations of  $E_0$  for eight LMC remnants are shown in Figure 8b, with [S II] measurements taken from Osterbrock and Dufour (1973), D'Odorico and Sabbadin (1976), and Dopita, Mathewson, and Ford (1977). The error bars indicate the range of permissible values for  $E_0(\text{optical})$  from equation (3) for those objects where observations at several positions have indicated largely different densities. (Note: If the range of observed densities for individual LMC remnants is real, it is quite different from the situation in our Galaxy, where only small changes of the [S II]  $\lambda 6717/\lambda 6731$  ratio are observed within individual SNRs; see Fesen, Blair, and Kirshner 1985.)

The optical LMC data in Figure 8b shows a correlation similar to that seen in Figure 7 for the M33 SNRs, although the scatter is larger. More directly, in Figure 8c we show the ratio  $E_0(\text{optical})/E_0(\text{X-ray})$  for the eight LMC remnants with both optical and X-ray data; there appears to be a trend toward higher values of this ratio for the larger remnants, although again the scatter is large. While a convincing claim for a real difference between the optical and X-ray determinations of  $E_0$  cannot be made with the present data, there is enough evidence to warrant a more thorough investigation.

Only one M33 SNR has been detected in X-rays, but it apparently confirms that a similar difference exists in M33. Markert and Rallis (1983) report *Einstein* high-resolution imager (HRI) data on M33, and their source M33 X-13 corresponds to D'Odorico, Dopita, and Benvenuti's (1980) SNR M33-9. Assuming  $f = 0.25$ ,  $T_x = 5 \times 10^6$  K, and  $\epsilon = 3 \times 10^{-23}$  as discussed above, and using equation (4), we find  $n_0 = 3.6 \text{ cm}^{-3}$  and  $n_x T_x = 7.2 \times 10^7 \text{ cm}^{-3} \text{ K}$ . Using  $N_e(\text{S II})$  from Table 5 and assuming  $\text{S}^+$  to be formed in a region of  $T \approx 10^4$  K, we find an optical pressure,  $n_{\text{op}} T_{\text{op}} = 1.7 \times 10^6 \text{ cm}^{-3} \text{ K}$ , a factor of  $\sim 40$  smaller than the X-ray pressure. We note that this is one of the smallest diameter M33 remnants, so it would be expected to show such a difference if indeed one exists.

#### b) Free Expansion or Sedov Evolution?

The evolutionary trends for a sample of SNRs can be investigated using a relationship between the number of SNRs less than or equal to some diameter,  $N(\leq D)$ , and diameter, viz.,

$$N(\leq D) = kD^\alpha, \quad (7)$$

where  $k$  and  $\alpha$  are constants related to the supernova rate and evolutionary state of the sample, respectively. This can be seen in the following way. Suppose that SNR evolution follows a power law,

$$D = D_0(t/t_0)^\delta, \quad (8)$$

where  $D_0$  is the SNR diameter at time  $t_0$ . Letting  $\tau$  be the interval between supernovae, we have

$$N(\leq D) = t(D)/\tau, \quad (9)$$

or, applying equation (8),

$$N(\leq D) = (t_0/\tau)(D/D_0)^{1/\delta}. \quad (10)$$

This can be further simplified by choosing  $t_0 = \tau$  and letting  $\alpha = 1/\delta$ , so that

$$N(\leq D) = (D/D_\tau)^\alpha, \quad (11)$$

where  $D_\tau = D(t = \tau)$ . In log format, we have

$$\log N(\leq D) = \alpha \log D - \alpha \log D_\tau. \quad (12)$$

This form of the cumulative number-diameter relation is particularly useful for investigating evolutionary trends. For instance, if a sample of remnants are in the free expansion phase (i.e., with  $D \propto t$ ), they should produce a distribution of SNRs with  $\alpha = 1$ . Alternatively, adiabatic expansion into a homogeneous medium (Sedov solution,  $D \propto t^{2/5}$ ; see Chevalier 1974) predicts  $\alpha = 2.5$ . Once the correct  $D(t)$  relation is established, then  $D_\tau$  can be used to determine the supernova rate. These parameters can be determined empirically from a plot of  $\log N(\leq D)$  versus  $\log D$ , where  $\alpha$  will be the slope and  $(-\alpha \log D_\tau)$  will be the intercept (see eq. [12]).

For years it has been thought that most galactic SNRs are expanding adiabatically, a view that has been supported by both radio surveys (Clark and Caswell 1976) and observations of deceleration in young historical remnants such as Tycho (Kamper and van den Bergh 1978), as well as theoretical arguments (Spitzer 1978). Values of  $\alpha \approx 2.5$  were also reported for SNRs in the LMC (Dennefeld 1978) and M31 (Dennefeld and Kunth 1981). However, using a more complete LMC sample derived from combined radio, X-ray, and optical techniques, Mathewson *et al.* (1983) recently found  $\alpha = 1.0 \pm 0.2$  for  $D \leq 50$  pc, which is consistent with free expansion.

In order to investigate M33 in this manner, we would like the sample of SNRs to be as complete as possible. In addition to the 19 candidates listed by D'Odorico, Dopita, and Benvenuti (1980), Sabbadin (1979) has compiled a separate list of 22 candidate SNRs from plates taken at Asiago. Only six of Sabbadin's objects are duplicated in the list of D'Odorico, Dopita, and Benvenuti (1980) (M33-4, M33-6, M33-7, M33-8, M33-9, and M33-11, respectively). Of the 19 candidates of D'Odorico, Dopita, and Benvenuti (1980), 13 have been confirmed spectroscopically, and inspection of the other six candidates on H $\alpha$  + [N II], [S II], and continuum plates of M33 obtained by us at McGraw-Hill Observatory confirms that these are very probably SNRs. The 16 additional candidates from Sabbadin (1979) have also been inspected on our plates; we find that only two of the 16 (Sabbadin's Nos. 13 and 18) appear to be strong SNR candidates. (Note: Sabbadin confirmed No. 13 spectroscopically.) Of the remaining 14 objects, we find only two or three which have marginally enhanced [S II] emission relative to H $\alpha$  on our plates, and these are probably low-excitation H II regions. Some of the objects also show some residual emission on the continuum photograph. Since Sabbadin (1979) makes no mention of a comparison with a continuum plate of M33, this could be the cause of part of the discrepancy. Also, if Sabbadin's [S II] plate was very deep, saturation effects could have caused the [S II]/H $\alpha$  ratio to be overestimated.

To summarize, there are 21 SNRs and probable SNRs in M33 with reasonably good optical diameter measurements (19 from D'Odorico, Dopita, and Benvenuti 1980 and Nos. 13 and 18 from Sabbadin 1979). The  $\log N(\leq D)$ - $\log D$  relation for this sample is shown in Figure 9. The solid line in Figure 9 is a least

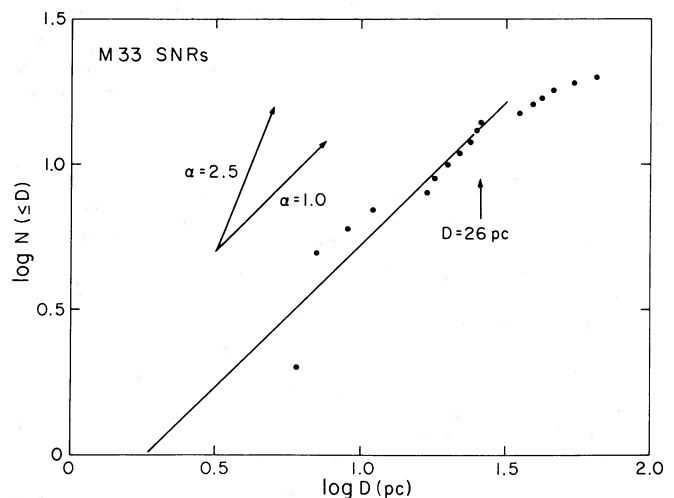


FIG. 9.—The cumulative number-diameter relation for M33 SNRs. The line is a least squares fit to the data with  $D \leq 26$  pc. Lines of slope 1.0 (free expansion) and 2.5 (Sedov model) are shown for comparison.

squares line fitted to the data below  $D = 26$  pc, where the sample appears to be reasonably complete, the formal parameters being

$$\log N(\leq D) = 0.976 \log D - 0.251, \quad (13)$$

which is very close to the expectation for free expansion (i.e.,  $\alpha = 1$ ), as found by Mathewson *et al.* (1983) in the LMC. Above  $D = 26$  pc, the sample may be incomplete owing to a bias against detecting large, low surface brightness remnants against the galaxy background (especially in the inner regions).

If the M33 remnants are really in free expansion to diameters of  $\sim 26$  pc, equations (12) and (13) can be solved for the supernova rate in M33. For free expansion,  $D_\tau = 2v\tau$ , where  $v$  is the ejection velocity in the supernova explosion. Mathewson *et al.* (1983) assume  $v = 5000 \text{ km s}^{-1}$  as the appropriate velocity (Patchett and Branch 1972), but  $s^{-1}$  as the appropriate velocity (Patchett and Branch 1972), but ejection velocities of typically  $12,000 \text{ km s}^{-1}$  are inferred from line widths in Type I supernovae (Kirshner *et al.* 1973; Kirshner and Kwan 1974). This uncertainty compromises the rate determination, with  $\tau \approx 74\text{--}178$  years corresponding to the above velocity range. The interval between supernovae will be even shorter than this if the sample below  $D = 26$  pc is incomplete, as it probably is. Several historical galactic remnants would have gone undetected at the distance of the LMC, for example, let alone at the distance of M33.

This supernova rate may be marginally at odds with the rate determined from extragalactic supernova statistics. Tammann (1977) gives the supernova rate for Sc galaxies as  $v_{\text{sin}} = 1.38 \pm 0.25$  per  $10^{10} L_\odot$  per 100 yr interval. Using  $B_0^2 = 5.79$  from de Vaucouleurs, de Vaucouleurs, and Corwin (1976) for M33 and a distance of 720 kpc,  $L(\text{M33}) = 0.36 \times 10^{10} L_\odot$ . Using  $v_{\text{sn}}$  from above, this implies  $\tau \approx 200(+45, -30)$  yr. Tammann (1978) gives a revised supernova rate for Sc galaxies which yields a somewhat higher value of  $\tau \approx 245$  yr. This difference may be large enough to cause some suspicion about the free-expansion argument. (We note in passing, however, that if the free-expansion argument is correct, thermalization of kinetic energy cannot be used to explain the  $E_0$ - $D$  correlation discussed in the previous section.)

### c) Sedov Evolution Revisited

Many of the assumptions in the free-expansion analysis can be questioned, although a quantitative analysis of possible deviations from these assumptions is difficult. For instance, the assumption of completeness of the sample to any given diameter is almost certainly not correct; any of a number of observational and environmental selection effects can conspire to cause many remnants to have been missed in current surveys. It is not likely, however, that incompleteness can account for the severe differences in the predictions of the  $N(\leq D)$ - $D$  relation for the free-expansion and homogeneous Sedov models.

The assumption of homogeneity involved in the Sedov model is not very realistic either. Even if conditions in the region surrounding a given remnant were approximately homogeneous, comparing a number of remnants from different positions within a galaxy almost guarantees inhomogeneity in the sample as a whole. In addition, since Sedov evolution is dependent on the supernova energy as well, any intrinsic spread in  $E_0$  for a sample of remnants will also affect the shape of the  $N(\leq D)$ - $D$  relation.

Hughes, Helfand, and Kahn (1984) have recently analyzed the LMC X-ray remnant sample with these considerations in

mind. In particular, the evolution of a remnant's luminosity with time (and hence with diameter) is a function of  $E_0/n_0$ . Hence, in a luminosity-limited sample, various remnants reach a given luminosity (say, the detection limit) at different diameters, depending on the range of variations of  $E_0/n_0$  within the sample. Using the X-ray limit for the *Einstein* imaging proportional counter (IPC) survey of the LMC and assuming a range of variation for  $E_0/n_0$  of  $10^5$ , Hughes, Helfand, and Kahn (1984) find that the observed  $N(\leq D)$ - $D$  relation for the LMC ( $\alpha \approx 1$ ) is consistent with *Sedov* evolution. (Note: the X-ray results shown in Fig. 8a imply that a range in  $E_0/n_0$  of  $\sim 10^4$  may be more appropriate.)

Applying these results to the M33 remnants is not straightforward. The M33 sample has been selected optically, and while an optical luminosity limit is no doubt present, its value is unknown and it varies with position in the galaxy. Nonetheless, similarities are expected between the interstellar media of Sc and irregular galaxies, and it seems likely that Hughes, Helfand, and Kahn's (1984) explanation for the LMC situation may also hold true for M33. We note that there is some tendency for the smaller diameter M33 SNRs to be located closer to the center of the galaxy or in spiral arms, while larger diameter remnants are found at greater galactocentric distances or in interarm regions. This could be attributed to variations in the mean values of  $n_0$  at various positions in M33 as well as selection effects.

## V. CONCLUSIONS AND FUTURE WORK

We have used improved optical spectra of SNRs in M33 to investigate abundance gradients and SNR evolution in this galaxy. Abundances of O, N, and S have been derived from the spectra using new shock models by Dopita *et al.* (1984). However, the O abundances may be affected by possible contamination from H II regions and low-velocity ( $\lesssim 100 \text{ km s}^{-1}$ ) shocks. The results for N and S show abundance gradients that are similar to the abundance gradients in NGC 300 and our own Galaxy.

The  $N(\leq D)$ - $D$  relation for M33 SNRs is consistent with a free-expansion model of evolution at least to a diameter of  $\sim 26$  pc. However, the recent analysis of LMC SNRs by Hughes, Helfand, and Kahn (1984) casts doubt on this interpretation, and Sedov evolution in regions of widely varying density may be more likely. The M33 SNRs show the same basic correlation between  $E_0$  and diameter that has been pointed out for other samples of SNRs when  $E_0$  is determined optically. X-ray observations of the M33 remnants would provide independent estimates of  $E_0$  for comparison with the optical results, and might allow the range of  $E_0$  and  $n_0$  for M33 remnants to be determined. Also, a consistent compilation of X-ray luminosities and pressure estimates for galactic remnants is needed for comparison with optical observations.

Spectra have been obtained for only 13 of the 21 SNR candidates in M33. Confirmation of the remaining objects is important both in terms of enlarging the sample for the abundance studies and for the evolutionary studies discussed in § III*d*. Some of these objects have very low surface brightnesses, and others lie close to H II regions, so these observations will be difficult. Long-slit observations may provide better data on those objects where H II region contamination is suspected.

Combined ultraviolet and optical spectra are much more powerful in conjunction with shock models than optical data alone. Ultraviolet spectra would allow the abundance of carbon to be obtained and would also permit the shock veloc-

ities of the remnants to be estimated. This would break the abundance/shock velocity ambiguity in the optical [O III] lines and allow more trustworthy determinations of the O abundances. All but the brightest M33 remnants are beyond the capability of the *International Ultraviolet Explorer* satellite, but observations with the Space Telescope would be very beneficial.

We would like to thank R. A. Fesen for reducing the KPNO and McGraw-Hill spectroscopic data, and N. Burnham for much assistance with the Mount Hopkins data reduction and analysis. This work was supported by NASA grant NAG 5-87 to the Smithsonian Astrophysical Observatory and NSF grant AST 83-09496 to the University of Michigan.

## REFERENCES

- Allain, D., Collin-Souffrin, S., Joly, M., and Vigroux, L. 1979, *Astr. Ap.*, **78**, 200.
- Benvenuti, P., Dopita, M. A., and D'Odorico, S. 1980, *Ap. J.*, **238**, 601.
- Binette, L., Dopita, M. A., D'Odorico, S., and Benvenuti, P. 1983, *Astr. Ap.*, **115**, 315.
- Blair, W. P., Kirshner, R. P., and Chevalier, R. A. 1981, *Ap. J.*, **247**, 879.
- . 1982, *Ap. J.*, **254**, 50.
- Blair, W. P., Raymond, J. C., D'Odorico, S., Benvenuti, P., and Dopita, M. A. 1985, in preparation.
- Butler, S. E., and Raymond, J. C. 1980, *Ap. J.*, **240**, 680.
- Chevalier, R. A. 1974, *Ap. J.*, **188**, 501.
- Clark, D. H., and Caswell, J. L. 1976, *M.N.R.A.S.*, **174**, 267.
- Cox, D. P. 1972a, *Ap. J.*, **178**, 143.
- . 1972b, *Ap. J.*, **178**, 159.
- Danziger, I. J., Murdin, P. G., Clark, D. H., and D'Odorico, S. 1979, *M.N.R.A.S.*, **186**, 555.
- Dennefeld, M. 1978, *Mem. Soc. Astr. Italiana*, **49**, 535.
- Dennefeld, M., and Kunth, D. 1981, *A.J.*, **86**, 989.
- de Vaucouleurs, G., de Vaucouleurs, A., and Corwin, H. G. 1976, *Second Reference Catalogue of Bright Galaxies* (Austin: University of Texas Press).
- de Vaucouleurs, G., and Pence, W. D. 1978, *A.J.*, **83**, 1163.
- Dickel, J. R., and D'Odorico, S. 1984, *M.N.R.A.S.*, **206**, 351.
- Dickel, J. R., D'Odorico, S., Felli, M., and Dopita, M. A. 1982, *Ap. J.*, **252**, 582.
- D'Odorico, S., Dopita, M. A., and Benvenuti, P. 1980, *Astr. Ap. Suppl.*, **40**, 67.
- D'Odorico, S., Goss, W. M., and Dopita, M. A. 1982, *M.N.R.A.S.*, **198**, 1059.
- D'Odorico, S., and Sabbadin, F. 1976, *Astr. Ap.*, **50**, 315.
- Dopita, M. A. 1977, *Ap. J. Suppl.*, **33**, 437.
- . 1978, *Ap. J. Suppl.*, **37**, 117.
- . 1979, *Ap. J. Suppl.*, **40**, 455.
- Dopita, M. A., Binette, L., D'Odorico, S., and Benvenuti, P. 1984, *Ap. J.*, **276**, 653.
- Dopita, M. A., Binette, L., and Schwartz, R. D. 1982, *Ap. J.*, **261**, 183.
- Dopita, M. A., D'Odorico, S., and Benvenuti, P. 1980, *Ap. J.*, **236**, 628.
- Dopita, M. A., Mathewson, D. S., and Ford, V. L. 1977, *Ap. J.*, **214**, 179.
- Draine, B. D., and Salpeter, E. E. 1979, *Ap. J.*, **231**, 438.
- Dufour, R. J., Schiffer, F. H., III, and Shields, G. A. 1984, in *The Future of Ultraviolet Astronomy Based on Six Years of IUE Research*, ed. Y. Kondo, R. D. Chapman, and J. M. Mead, in press.
- Dufour, R. J., Talbot, R. J., Jr., Jensen, E. B., and Shields, G. A. 1980, *Ap. J.*, **236**, 119.
- Evans, I. N., and Dopita, M. A. 1985, *Ap. J.*, submitted.
- Fesen, R. A., Blair, W. P., and Kirshner, R. P. 1982, *Ap. J.*, **262**, 171.
- . 1985, *Ap. J.*, in press.
- Fesen, R. A., and Kirshner, R. P. 1980, *Ap. J.*, **242**, 1023.
- Goss, W. M., Ekers, R. D., Danziger, I. J., and Israel, F. P. 1980, *M.N.R.A.S.*, **193**, 901.
- Hartmann, L., and Raymond, J. C. 1984, *Ap. J.*, **276**, 560.
- Hawley, S. A., and Grandi, S. A. 1977, *Ap. J.*, **217**, 420.
- Hester, J. J., Parker, R. A. R., and Dufour, R. J. 1983, *Ap. J.*, **273**, 219.
- Hughes, J. P., Helfand, D. J., and Kahn, S. M. 1984, *Ap. J. (Letters)*, **281**, L25.
- Kamper, K. W., and van den Bergh, S. 1978, *Ap. J.*, **224**, 871.
- Kirshner, R. P., and Kwan, J. 1974, *Ap. J.*, **193**, 27.
- Kirshner, R. P., Oke, J. B., Penston, M. V., and Searle, L. 1973, *Ap. J.*, **185**, 303.
- Kwitter, K. B., and Aller, L. H. 1981, *M.N.R.A.S.*, **195**, 939.
- Latham, D. 1982, in *IAU Colloquium 67, Instrumentation for Astronomy with Large Optical Telescopes*, ed. C. M. Humphries (Dordrecht: Reidel), p. 259.
- Long, K. S. 1983, in *IAU Symposium 101, Supernova Remnants and Their X-Ray Emission*, ed. J. Danziger and P. Gorenstein (Dordrecht: Reidel), p. 525.
- Long, K. S., Helfand, D. J., and Grabelsky, D. A. 1981, *Ap. J.*, **248**, 925.
- Markert, T. H., and Rallis, A. D. 1983, *Ap. J.*, **275**, 571.
- Mathewson, D. S., and Clarke, J. N. 1972, *Ap. J. (Letters)*, **178**, L105.
- Mathewson, D. S., Ford, V. L., Dopita, M. A., Tuohy, I. R., Long, K. S., and Helfand, D. J. 1983, *Ap. J. Suppl.*, **51**, 345.
- Mathewson, D. S., Ford, V. L., Dopita, M. A., Tuohy, I. R., Mills, B. Y., and Turtle, A. J. 1984, *Ap. J. Suppl.*, **55**, 189.
- McKee, C. F., and Cowie, L. L. 1975, *Ap. J.*, **195**, 715.
- Mendoza, C., and Zeppen, C. J. 1982, *M.N.R.A.S.*, **198**, 127.
- Miller, J. S., and Mathews, W. G. 1972, *Ap. J.*, **172**, 593.
- Mills, B. Y., Little, A. G., Durdin, J. M., and Kesteven, M. J. 1982, *M.N.R.A.S.*, **200**, 1007.
- Oke, J. B. 1974, *Ap. J. Suppl.*, **24**, 21.
- Osterbrock, D. E. 1974, *The Astrophysics of Gaseous Nebulae* (San Francisco: Freeman).
- Osterbrock, D. E., and Dufour, R. J. 1973, *Ap. J.*, **185**, 441.
- Pagel, B. E. J., and Edmunds, M. G. 1981, *Ann. Rev. Astr. Ap.*, **19**, 77.
- Pagel, B. E. J., Edmunds, M. G., Blackwell, D. E., Chun, M. S., and Smith, G. 1979, *M.N.R.A.S.*, **189**, 95.
- Pagel, B. E. J., Edmunds, M. G., and Smith, G. 1980, *M.N.R.A.S.*, **193**, 219.
- Patchett, B., and Branch, D. 1972, *M.N.R.A.S.*, **158**, 375.
- Peimbert, M., and Torres-Peimbert, S. 1977, *M.N.R.A.S.*, **179**, 217.
- Pradhan, A. K. 1978, *M.N.R.A.S.*, **183**, 89P.
- Raymond, J. C. 1979, *Ap. J. Suppl.*, **39**, 1.
- Raymond, J. C., Black, J. H., Dupree, A. K., Hartmann, L., and Wolf, R. S. 1980, *Ap. J.*, **238**, 881.
- . 1981, *Ap. J.*, **246**, 100.
- Raymond, J. C., and Smith, B. W. 1977, *Ap. J. Suppl.*, **35**, 419.
- Sabbadin, F. 1979, *Astr. Ap.*, **80**, 212.
- Seab, C. G., and Shull, J. M. 1983, *Ap. J.*, **275**, 652.
- Searle, L. 1971, *Ap. J.*, **168**, 327.
- Seward, F. D., and Mitchell, M. 1981, *Ap. J.*, **243**, 736.
- Shaver, P. A., McGee, R. X., Newton, L. M., Danks, A. C., and Pottasch, S. R. 1983, *M.N.R.A.S.*, **204**, 53.
- Shectman, S. A., and Hiltner, W. A. 1976, *Pub. A.S.P.*, **88**, 960.
- Shull, J. M., and McKee, C. F. 1979, *Ap. J.*, **227**, 131.
- Smith, H. E. 1975, *Ap. J.*, **199**, 591.
- Spitzer, L. 1978, *Physical Processes in the Interstellar Medium* (New York: Wiley), p. 255.
- Stasinska, G., Alloin, D., Collin-Souffrin, S., and Joly, M. 1981, *Astr. Ap.*, **93**, 362.
- Talent, D. L., and Dufour, R. J. 1979, *Ap. J.*, **233**, 888.
- Tammann, G. A. 1977, in *Supernovae*, ed. D. N. Schramm (Dordrecht: Reidel), p. 95.
- . 1978, *Mem. Soc. Astr. Italiana*, **49**, 315.
- van Speybroeck, L., Epstein, A., Forman, W., Giacconi, R., Jones, C., Liller, W., and Smart, L. 1979, *Ap. J. (Letters)*, **234**, L45.
- Whitmore, B. C. 1984, *Ap. J.*, **278**, 61.

WILLIAM P. BLAIR: Department of Physics and Astronomy, The Johns Hopkins University, Baltimore, MD 21218

ROBERT P. KIRSHNER: Department of Astronomy, University of Michigan, Ann Arbor, MI 48109-1090